LAWRENCE
LIVERMORE
NATIONAL
LABORATORY

Prospects for high-gain, high yield National Ignition Facility targets driven by 2(omega) (green) light

L. J. Suter, S. Glenzer, S. Haan, B. Hammel, K. Manes, N. Meezan, J. Moody, M. Spaeth, L. Divol, K. Oades, M. Stevenson

December 18, 2003

Disclaimer

Prospects for high-gain, high yield National Ignition Facility targets driven by 2ω (green) light

L. J. Suter, S. Glenzer, S. Haan, B. Hammel, K. Manes, N. Meezan, J. Moody. M. Spaeth, L. Divol *Lawrence Livermore National Laboratory, University of California, Livermore, CA 94551*

K. Oades, M. Stevenson *Atomic Weapons Establishment, Aldermaston, UK*

The National Ignition Facility (NIF) (J. A. Paisner, E. M. Campbell and W. J. Hogan, Fusion Technol. **26**, 755 (1994)), operating at green (2ω) light, has the potential to drive ignition targets with significantly more energy than the 1.8 MJ it will produce with its baseline, blue (3ω) operations. This results in a greatly increased "target design space", providing a number of exciting opportunities for fusion research. These include the prospect of ignition experiments with capsules absorbing energies in the vicinity of 1 MJ. This significant increase in capsule absorbed energy over the original designs at ~150 kJ could allow high-gain, high yield experiments on NIF. This paper reports the progress made exploring 2ω for NIF ignition, including potential 2ω laser performance, 2ω ignition target designs and 2ω Laser Plasma Interaction (LPI) studies.

I- Introduction

For several years we have been exploring the possibility of using green (2ω) light for indirect drive ignition on the National Ignition Facility (NIF). The rationale for this work is the possibility of extracting significantly more energy (~2X) from NIF in green light, as compared to blue (3ω) light, and driving far more energetic capsules than we originally envisioned when we started planning NIF in the early 1990's. This paper attempts to provide a comprehensive picture of the progress we have made exploring 2ω for NIF ignition. First we describe the potential operating regime for NIF at 2ω and how that can translate into a very large "design space" for exploring ignition target designs. We then present the results of 2ω ignition target design studies indicating that we can achieve adequate drive and symmetry with 2ω and show how we might capitalize on the large amount of energy available by electing to trade-off coupling efficiency for, say, better symmetry or plasma conditions. These simulations also define plasma conditions for ignition-relevant 2ω Laser-Plasma Interaction (LPI) experiments that have been recently performed. We summarize the results of these experiments using modern beam smoothing techniques which indicate that 2ω LPI is not fundamentally different from 3ω's. Finally, we show how recent experimental findings on mitigating 2ω laser plasma interactions through reduced intensity and/or judicious choice of plasma composition can be incorporated into ignition target designs.

II- Potential target design space available with 2ω

The fundamental requirements of the National Ignition Facility Laser now being constructed at Lawrence Livermore National Laboratory include that it shall be capable of irradiating a target with 1.8MJ of 0.35μm (3ω or "blue") light in an ignition pulse shape peaking at 500TW. The 3ω light is produced by a neodinium phosphate glass laser system [1] which first produces infrared or "1ω" light of 1.053μm wavelength which is then converted to 3ω light by a pair of KDP crystals [2]. The crystals combine three 1ω

photons into one 3ω photon. Ignition pulse shapes require peak power after a long, low power "foot" lasting many nanoseconds. Moreover, this peak power must be produced after a significant amount of energy has already been extracted from the $1\mu m$ laser since crystals tuned to provide optimum, ~70% conversion of 1ω to 3ω at peak power have relatively low conversion during the foot. Since the average conversion efficiency for a 3ω ignition pulse shape, without any advanced conversion schemes, works out to be about 50%, NIF's "$1\mu m$ engine" was designed to produce ~700TW of 1ω power after >3MJ of $1\mu m$ energy has been extracted. The consequence of this is that NIF's $1\mu m$ laser is necessarily very much larger than the 1.8MJ specified output. Figure 1 shows current estimates of NIF's maximum performance, plotting the peak 1ω power that the laser can produce as a function of the 1ω energy extracted from the laser. It indicates that NIF's peak, extractable 1ω energy would be ~6.5MJ. This estimate is for NIF's so-called 11-7 configuration with all seven "slots" in the final, booster amplifiers loaded with slabs of neodynium glass. We note that at this writing the first four beams of NIF have already demonstrated [3] 104kJ of $1\mu m$ light output, equivalent to 5MJ of 1ω from full 192 beam NIF.

Previously [4] we discussed how 3ω operations at lower powers, in tandem with improvements in hohlraum coupling efficiency, might allow NIF to drive capsules that absorb ~400-600kJ. In this paper we present an assessment of the possibilities offered by operating NIF as a green, 2ω laser and show how it allows ignition and, even, high yield opportunities far beyond what we originally envisioned when we started NIF in the early 90's. NIF's potential for driving ignition targets with 2ω can be simply estimated by $E_{cap}=E_{1\omega}*(\eta_{1-2})*\eta_H$, where E_{cap} is the capsule absorbed energy, $E_{1\omega}$ is NIF's maximum 1ω output (~6.5MJ), η_{1-2} is the conversion efficiency of 1ω laser energy to 2ω (~80-85% average conversions to green are possible) and η_H is the hohlraum coupling efficiency. This gives E_{cap}~5MJ*η_H, or capsules absorbing >~1MJ energy at plausible hohlraum coupling efficiencies of 20-25% [4].

Figure 2 summarizes a more detailed analysis and graphically shows NIF's potential "ignition target design space" with 2ω. It plots NIF energy vs. capsule absorbed energy. The light and darker shaded areas show target design space potentially available with 2ω at 250eV peak radiation temperature and 300eV peak radiation temperature, respectively. We refer to this as target design spaces because it illustrates all the combinations of NIF energy and capsule energy where an ignition target might be designed at a given peak radiation temperature. Both these design spaces are very much larger than the design space we originally envisioned in ~1991 when we began NIF, shown by the dark triangle in the lower left section.

To better appreciate the target design space plots of figure 2 and to understand how they are developed we begin by noting that the light grey, dotted lines are lines of constant hohlraum coupling efficiencies, η_H. The bold lines bounding the right hand sides of the 250eV and 300eV design spaces are estimates of coupling efficiency for cylindrical NIF ignition hohlraums with a "standard" case:capsule ratio=(hohlraum area/capsule area)$^{1/2}$ of 3.65 [4]. These efficiencies have a slight non-linearity, $\sim(E_{cap})^{0.1}$. The left hand, vertical boundaries indicate estimated minimum energy of ignition at a given peak radiation temperature. The boundaries drawn combine the approximate minimum energy of ignition at 300eV, generally taken to be ~100kJ, and the $T_R^{4.5}$ scaling for minimum energy developed by Lindl, [5] assuming "similar" targets. We note, however, that the minimum energy for ignition can be significantly affected by target design and is the subject of ongoing research. For example Dittrich [6] has designed a capsule which, at 250eV, also has a minimum energy of ignition of ~100kJ.

The upper bound of target design space is found at each hohlraum coupling efficiency by combining target pulse shape requirements with the conversion efficiency, η_{1-2}, of 1ω to 2ω light and NIF's 1ω performance curve, figure 1. The procedure is as follows: Target pulse shape requirements are derived from the x-ray power vs. time absorbed by a given capsule. Figure 3 shows the x-ray power absorbed by a 600kJ, 250eV graded dopant Be capsule designed by Haan in 1991 (designated "Haan'91") [4]. We readily scale this capsule's x-ray power requirements, P_{cap0}, to other absorbed energies via a capsule

4

scaling parameter "s". Multiplying P_{cap0} by s^2, time by s, and all the dimensions of the capsule by s, scales capsule absorbed energy by s^3 or $E_{cap}=600kJ*s^3$ for this scaled capsule. For a given E_{cap} the 2ω pulse shape requirement is simply (x-ray power absorbed by the capsule)/(hohlraum coupling efficiency)= P_{cap}/η_H . The 1ω power produced by the laser must then be $P_{1\omega}=P_{cap}/(\eta_H \eta_{1-2})$. However, figure 1 provides a constraint on the maximum 1ω power, requiring $P_{1\omega} =P_{cap}/(\eta_H \eta_{1-2})< P_{max}(E_{1\omega})$ where $E_{1\omega} =\int_0^t P_{1\omega}dt$. To find an upper bound at a given η_H and η_{1-2} we vary the capsule scale size parameter, s, until there is a point in the pulse shape where $P_{cap}/(\eta_H \eta_{1-2})=P_{max}(E_{1\omega})$.

Figure 4 plots these upper bounds for 250eV and 300eV peak radiation temperatures for 1ω to 2ω conversion efficiencies, η_{1-2}, ranging between 50 and 90%. Note that the upper bounds have a significant dependence on peak radiation temperature and on 1ω to 2ω conversion efficiency. The notable difference between the 300eV and 250eV upper bounds is because 300eV capsules require about twice the power of the 250eV capsules. 300eV targets are always power limited. It is not unreasonable to think of 250eV as marking the approximate boundary between designs limited by available power and ones limited by available energy. Analysis at 215eV, approximately a factor of 2 down in power requirement from 250eV, shows a design space only slightly larger than the 250eV space. At 215eV the targets are mostly limited by the 1ω energy available (giving a flat upper bound in the $E_{NIF} E_{CAP}$ plot), except at the lowest hohlraum coupling efficiencies where they, too, become power limited. We also note that at 300eV, 50% 1ω to 2ω conversion efficiency, the design space is not very much larger than the one we originally envisioned for 300eV NIF targets.

Figure 2 shows an ignition target design space using 2ω that is far greater than the target design space that existed in the early '90s, when we first started thinking about NIF. At 300eV the increase comes principally from increased conversion efficiency, an increase in our expected coupling efficiency [4] and a clearer understanding of how the 1ω laser will operate. Further expansion of target design space comes from operating at 250eV

rather than 300eV, where the power requirements as a function of extracted energy are better matched to NIF's 1ω capabilities. In order to achieve this performance considerably more green energy must pass through NIF's final optics assembly (FOA) than the 8J/cm^2 of blue light that will pass through the FOAs during a 1.8MJ 3ω shot. Although this fluence currently defines the state-of-the-art damage limit for 3ω optics it is expected that approximately a factor of two higher fluences will be possible with green light, compared to blue, without damaging the FOAs. Current thinking is that if full NIF were available today it could reasonably produce between 3 and 4MJ of green light. With further optics research it is conceivable that 2ω optics could allow access to the entire design space.

III- Discussion: Benefits of larger design space and 2ω target physics concerns

The preceding section showed that NIF, operating at 2ω, has the potential to greatly increase target design space compared to our original expectations. This increase is desirable for several reasons. First, it allows us to contemplate capsules absorbing far more energy than we originally envisioned. Capsules absorbing ~100kJ (200kJ) are on the threshold of failure at 300eV (250eV) because of their small size [5,4]. Basically, as a given ignition capsule is scaled down in size and energy, heat conduction losses play an increasing dominant role in the hotspot power balance, causing 1-D estimates of yield vs. absorbed energy to have a very steep section or "cliff" at low energies. Significantly increasing capsule absorbed energy moves us away from this cliff. Increased capsule absorbed energy is also beneficial because a given capsule's ability to withstand surface roughness, which seeds hydrodynamic instabilities, increases very dramatically with absorbed energy [7]. Such important increases in margin, possible with increased capsule absorbed energy, would greatly increase our confidence in achieving ignition and allow us to consider studies of capsule physics and thermonuclear burn physics that are implausible with marginal capsules. A second reason the increase in design space is attractive is that it allows us to consider a wider range of possible hohlraums and to consider the possibility of trading-off capsule absorbed energy for something desirable such as better symmetry or improved diagnostic access.

The increase in target design space potentially available with 2ω makes it appear to be a desirable option for NIF. Unfortunately, virtually all the target physics studies that established the technical basis for NIF ignition [5,8] were done with 3ω light. When we first recognized the possibilities of green light no significant 2ω database existed. In order to redress this we have been working for several years to answer questions related to using 2ω light on NIF for ignition. This work has been divided into three major areas.

1- Laser operations: What performance might we get from NIF at 2ω and how might we actually operate NIF at 2ω. The previous section described the ignition performance we might get with 2ω. Work assessing 2ω operations is ongoing within the NIF project and will be reported elsewhere.

2- Projected 2ω ignition target performance assuming Laser Plasma Interactions are under control. In the next section we describe the result of integrated Lasnex simulations of large 2ω ignition targets.

3- Experimental studies of LPI issues for which there is no theoretical predictive capability. The key issues are 2ω propagation, 2ω backscatter and 2ω hot electron production. We have been studying these on both the Helen laser and Omega laser. We summarize current findings in section V.

IV- Lasnex studies of 2ω ignition targets

The large target design space potentially available with 2ω light gives us the luxury of being able to consider a wide range of ignition possibilities with Lasnex. Referring to the 250eV design space of figure 2, we have done integrated Lasnex simulations [9] of two targets that require ~3.5 MJ of green light. One target, with a standard case:capsule ratio of 3.65, lies on the limiting hohlraum coupling efficiency line, driving a capsule that absorbs ~850 kJ of x-rays. A second target demonstrates one of the trade-offs made possible by a very large target design space. It contains a capsule that absorbs only 400 kJ of x-rays, allowing us to increase the case:capsule ratio to 5.

7

Figure 5 shows the two targets we simulated with Lasnex. The target with standard, 3.65 case:capsule ratio has a Be "Haan'91" capsule ~4mm outer diameter placed inside an ~1cm diameter cocktail hohlraum [4,10,11,12]. This hohlraum is ~1.74X the size of the NIF point design [13]. The capsule absorbs 850kJ. In the other target is a scaled version of the same capsule with a diameter of ~3mm. It is inside a cocktail hohlraum ~1.1cm in diameter (scale 1.93), giving a case:capsule ratio of 5.0 and a capsule absorbed energy of ~400kJ. The 2ω pulse shapes we used in simulating the two targets are plotted in figure 6. Both are continuous pulse shapes of approximately 3.5 MJ. The target with larger case:capsule ratio requires higher power because its smaller capsule implodes more quickly; the ~same amount of energy must come in a shorter time. As in the original point designs, both targets include a low-Z gas fill (1mg/cc He) to retard the inward motion of the high-Z hohlraum walls in order to maintain symmetry [13,14]. We used typical NIF beam pointing as originally developed by Pollaine [13]. A variety of spot sizes were explored in the integrated simulations, including spots as large as ~4mm major diameter by ~1.5mm (3mm) minor diameter for the 44.5^{o}&50° (23°&30°) beam cones. Spots this large are closely matched to the laser entrance hole (LEH) size thereby minimizing intensity at the LEH. Integrated simulations with these "big spots", whose marginal rays come as close to the LEH as 400-550μm, give results very similar to simulations with considerably smaller spots. Using the large spot size with the 850kJ capsule's pulse shape gives a peak single-quad intensity of ~3×10^{14} w/cm^2 (~1.5×10^{14} w/cm^2) for quads on NIF's outer (inner) cones.

Extensive, 2D integrated Lasnex simulations indicate 2ω is very promising for igntion. The calculations, using the large spots just described, produce the desired $T_R(t)$ in the hohlraum. Indeed when we perform an identical simulation, except replacing 2ω with 3ω, we find nearly identical $T_R(t)$ profiles. The small differences can be attributed to slightly higher temperature of the hohlraum's coronal plasma with 2ω. We find that the simulated 2ω beams propagate to the walls and that we can control symmetry in the usual way, by moving the beams and/or adjusting the relative powers [13,14]. Consequently, we produce adequate symmetry and the capsules ignite and burn in our 2ω integrated simulations. The 850kJ capsule produces ~120 MJ and the 400 kJ capsule produces ~50

MJ. Both these yields are close to the 1D yields for these particular capsules driven by idealized $T_R(t)$ pulse shapes.

Figure 7 illustrates hotspot shape at ignition time for the two case:capsule ratios. We define ignition time as when the thermonuclear yield rate rises through ~2000TW, a useful rule-of-thumb criteria. At standard case:capsule ratio we see a hotspot shape that is very familiar from 3ω design work; a well formed hotspot showing evidence of an incipient jet of cold deuterium-tritium (DT) fuel on the pole together with an incipient curtain of cold DT fuel coming in around the waist of the capsule. Neither perturbation is sufficiently large to affect ignition (indeed, we find at these large absorbed energies that many poorly tuned targets with very much bigger jets and/or curtains will also ignite on the code). At larger case:capsule ratio we see evidence of a trade-off worth further exploration. The symmetry appears to have been improved. This hotspot shows no evidence of a budding pole jet or waist curtain. In tuning the symmetry we find that with these bigger capsules we can achieve adequate symmetry without needing time dependent "beam phasing". That is, without continuously and carefully varying the ratio of inner beam power to outer beam power to minimize time dependent variations in the P2 Legendre component of asymmetry [13,14]. For a given pointing, one, fixed in time ratio is adequate. That is not to say that with increased coupling energy we still wouldn't want to try to improve symmetry via some beam phasing. The fact that we don't necessarily need to use beam phasing in successful integrated simulations is an anecdotal measure of increased robustness due to increased absorbed energy.

The weakness of the design simulations just discussed is that neither Lasnex nor any other model can quantitatively predict LPI processes in the complex environment of an ignition hohlraum other than, perhaps, the onset of filamentation. In creating the technical basis for NIF we dealt with this shortcoming by doing a wide variety of Nova underdense interaction studies [15, 16,17, 5, 8] in targets we considered to be "ignition plasma emulators". That is, targets in which we had created, to the degree possible, plasma conditions similar to what we expect in ignition targets. Lasnex integrated simulations of ignition targets defined those plasma conditions. The plasma conditions from our

9

integrated simulations of the 250eV ignition target at 3.65 case:capsule ratio, at 1ns after peak power are plotted in figure 8 for the inner and outer cones. According to these plots, LPI for the outer beam principally involves a beam of $\sim 3\times 10^{14}$ W/cm^2 interacting with a low-Z plasma with Te~4keV and electron density ~0.1 to $0.14 n_c$, where n_c is the critical density for green light, 4×10^{21} electrons/cm^3. For the inner beams, LPI occurs at a lower intensity, ~1.5×10^{14} W/cm^2, and in a plasma that changes from He fill-gas to Be ablator blow-off about midway in the beam's path. The plasma density along this path ranges from ~0.1 to $0.2 n_c$. These conditions, then, determine the conditions for empirical studies of laser plasma interactions in a 2ω ignition target and how we might control them.

Ponderomotive filamentaion in these conditions can be estimated using a figure of merit. According to both theory and simulation [18] filamentation of NIF's f/8 beams will begin to occur when the filamentation figure of merit (FFOM)

$$I\lambda^2(n_e/n_c)(3/Te)>1\times 10^{13} \qquad (1)$$

and will have a very noticeable effect when the FFOM begins to exceed 2×10^{13}. In this expression I is laser intensity (W/cm^2), λ is wavelength (μm) n_e/n_c is the ratio of electron density to critical density and Te is electron temperature in keV. For the plasma conditions shown in figure 8, the FFOM at the LEH is 2.5×10^{12} (5×10^{12}) for the inner (outer) beams and peaks at 4×10^{12} (6×10^{12}) 6mm (5mm) inside the hohlraum as measured along the beam path from the LEH. These values indicate the 250eV, 2ω design will be below the threshold for filamentation.

V- Experimental studies of 2ω Laser Plasma Interaction (LPI)

The key underdense interaction issues for 2ω are essentially the same as they are for 3ω; propagation, backscatter and hot electron production. For 3ω ignition these issues were studied on the Nova laser during the 1990's as part of the Nova Technical Contract [5,8] that created the target physics basis for ignition with a NIF class facility. Of these issues, backscatter losses were the greatest concern and were studied in depth while hot electron production, which had never been observed to be large with 3ω, was monitored on Nova but never became the focus of detailed experiments.

In order to establish a database for laser plasma interactions at 2ω we have been studying underdense interactions on the 2ω Helen laser at the Atomic Weapons Establishment (AWE) [19] since 2000 and have converted one beam of the Omega laser at University of Rochester [20] to operate at 2ω [21]. We have been shooting green interaction experiments at Rochester since June, 2002.

The 2ω Omega experiments have principally studied backscatter and are described in greater detail by Moody [22]. Conceptually, the Omega studies are very similar to underdense interaction experiments carried out on Nova to study 3ω. They use a so-called "gasbag" target comprised of two thin (~3500A) polyimide membranes glued to either side of an aluminum washer which also has tiny tubes for filling the target with gas. When pressurized, the membranes stretch, forming an oblate spheroid of major diameter ~2.75mm and minor diameter ~2.2mm. These gasbags are heated by 1ns pulses from 40 of Omega's beams. The heater beams are defocussed to low intensity, nearly filling the bag's diameter and create a plasma with Te~ 2.5keV and scalelength >1mm. This plasma then "probed" by Omega's single 2ω beam which has ~400J in a 1ns pulse. The 2ω probe beam is smoothed by a phase plate which forms a spot that can achieve intensities up to $\sim 1 \times 10^{15}$ w/cm^2. Backscatter into the f/6 lens, the principal quantity studied, is measured by Omega's Full Aperture Bacscatter Station (FABS). At this point, Omega does not yet have a Near Backscatter Imaging diagnostic (NBI) to measure 2ω light scattered just outside the lens. Figure 9 shows one of the scalings we have performed on Omega. It plots 2ω stimulated Raman and stimulated Brillouin reflectivity as a function of intensity from gasbags filled with hydrocarbon gas to a density corresponding to 0.12nc of green light when the gas is fully ionized. We make several observations from this plot. First, hydrocarbon gasses at 2ω, like 3ω, mainly produce Raman backscatter at 0.12 nc. Second, the peak stimulated Raman backscatter into the lens at intensity approaching 10^{15} is ~15%, a typical value for 3ω light at similar conditions. Third, there is a clear intensity scaling to the backscatter that could be interpreted as a threshold for stimulated Raman at low-10^{14} w/cm^2.

A threshold for Raman backscatter at low-10^{14} W/cm^2 is encouraging because it can be explained by a filamentation argument and support for that explanation can be found in the data. At the heart of the filamentation argument is an assumption that Raman backscatter is produced mostly in the hotspots that form when the beam filaments. That is, if the beam filaments we get Raman backscatter but if the beam doesn't filament then Raman should be low. In these experiments simple theory and simulations with our laser plasma interaction code pF3D [23] indicate a threshold for filamentation around $3x10^{14}$ W/cm^2. This threshold is supported experimentally by a very narrow Raman backscatter spectrum at $3x10^{14}$ but very obviously broad Raman backscatter spectra at the higher intensities. (Broad Raman spectra are indicative of filamentation while a narrow spectrum is indicative of little or no filamentation). If the filamentation threshold hypothesis is correct, then this scales favorably to 2ω NIF ignition targets since, according to equation 1, the intensity threshold for filamentation should scale like ~Te. In Lasnex simulations of 2ω ignition targets Te is ~4.5keV, vs. ~2.5keV in these Omega experiments.

Complementing 2ω interaction experiments on Omega have been a wide ranging series of underdense interaction experiments using a single, ~400J/1ns 2ω beam on the Helen laser at AWE. The experiments mostly involved gasbag targets irradiated along the axis of symmetry by a phase-plate smoothed, 2ω spot, typically ~$6x10^{14}$ w/cm^2. A number of small, gas filled hohlraums were also shot, as well. The experiments are described in detail in a paper by Stevenson [24]. Here we summarize the three most important Helen findings on underdense interaction.

1- Propagation: Because the gasbag targets were irradiated by a single beam, we were able to study 2ω propagation via time resolved, side-on x-ray imaging. These side-on images show the formation of well defined plasma columns and closely match synthetic images from simulations with our radiation hydrodynamics code HYDRA [25]. We interpret the good agreement between experimental and synthetic images [26] as evidence that a 2ω beam can propagate in a manner consistent with straightforward hydrodynamics and evidence that, for backscatter production, these targets produced the long scalelength plasmas we expected from simulations.

2- Effect of composition on backscatter: Helen's seminal contribution to LPI is the discovery that plasma composition influences backscatter far more than was previously thought [24]. The black bars on figure 10 show stimulated Raman and Brillouin backscatter from the Helen gasbag targets as a function of composition, ordered in increasing average atomic number, Z. The vertical extent of a bar indicates the range of backscatter we measured from all targets filled with a given composition. At low Z we see the expected interchange of stimulated Raman for stimulated Brillouin when we switch from a composition with strong ion damping (C_5H_{12}) to a composition with weak ion damping (N_2, CO_2, Ne). This is consistent with Nova results [27]. The unexpected finding was the drop in Brillioun with rising Z and the fact that Raman remained low even as Brillouin dropped. This was inconsistent with a widely held view of an interplay between Raman and Brillouin and that reduction of one results in the increase of the other. These findings have been reproduced in subsequent Omega gasbag experiments using 40 heater beams and one probe. The grey bars in figure 10 plot the Omega results.

3- Control of hot electron production: Historically, hot electron production was the bane of early attempts to do ICF with lasers having wavelengths of 1μm or longer. For example, experiments on the 1μm Shiva laser showed hot electron production to rise as hohlraums are driven to higher energy density and that in the highest energy density hohlraums it was possible to convert >20% of the laser energy to hot electrons with an ~50keV Maxwellian distribution. Such high hot electron fractions prevent ignition by preheating the DT fuel. The discovery in the early '80's that shorter wavelengths suppress hot electron production led the community to build subsequent facilities to operate at the shortest wavelength technically feasible, i.e. 3ω. Long experience has justified that decision. Empirically, 3ω does not efficiently make hot electrons. When considering the possibility of using 2ω, history cautions to be wary of the specter of hot electrons. This where Helen experiments have made a second original contribution to LPI; hot electron production and how to control it. Measurements of time integrated, absolute hard x-ray production with Helen's Filter Fluourescer diagnostic (FFLEX) allow us to infer hot electron production. In gasbag targets, we find that C_5H_{12} fills, which efficiently produce stimulated Raman

backscatter, also produce a rising hot electron fraction as a function of fill density, peaking near fills of $0.25n_c$. However, when we switch to other gasses, which do not produce much Raman, the hot electron signal remains relatively low, even as the fill density approaches $0.25n_c$ [24]. This indicates that plasma composition can control hot electron production, just as it appears to control backscatter. These Helen experiments suggest two rules-of-thumb for designing 2ω ignition targets with low hot electron production. Keep most of the LPI volume below 0.15nc and/or judiciously choose materials to avoid Raman producers.

VI- Alternative ignition hohlraum designs

The finding that we can control backscatter and hot electron production via judicious choice of plasma composition is potentially very important for NIF because it implies that we can control LPI via target design. This has engendered a new area of target design, exploring targets where the conventional He/H gas-fill of an ignition point [13,14] is replaced by other materials. A constraint on these designs is a preshot temperature of $\sim18^{o}K$ needed for the cryogenic capsule. This eliminates most gasses since they would freeze out.

Our exploration of alternative hohlraum designs has been exclusively on variants of the standard case:capsule ratio target of figure 5, using the pulse shape shown by the solid line of figure 6 and the 850 kJ Be capsule. Our investigations fall into two cryogenic-compatible classes; designs where the He gas fill is replaced by a foam and designs where it is largely replaced by a mid-Z or high-Z liner. In the foam designs we replaced the 1mg/cc He gas by 1mg/cc SiO_2 (this foam exists) or 1mg/cc GeO_2 and, even, 1mg/cc XeO_2 (this foam cannot exist but allows us to study the scaling with Z). The lined targets we studied included hohlraums lined with $1\mu m$ solid (frozen) Kr and $1\mu m$ frozen Xe.

The result of these integrated simulations is that it appears possible to replace the He or He-H gas in NIF hohlraums with mid to high Z material and still maintain drive and symmetry adequate for ignition. The calculated $T_R(t)$ from hohlraum simulations using

14

the three different foams are close to what is calculated for He fill. The simulated hotspot shapes at ignition do not look very much different than the one found with He fill, in figure 7. The capsules work in these integrated simulations, producing yields ~120MJ, similar to He filled targets. It was not necessary to make any design changes compensating for the increased x-ray preheat of the higher-Z foams. The principal drawback is that the hohlraum has a greater propensity to produce a pole high implosion as we raise the average Z of the fill. In this study we counteracted this tendency by switching a greater fraction of the laser power to the inner beams. If the pole-high tendency cannot be offset by some other change, such as geometry, this might limit the upper bound to the Z of the foam.

In addition to the foam simulations, we also investigated replacing the He gas with $1\mu m$ liners of either Kr or Xe. Although these designs readily produced the required $T_R(t)$, we were unable to find a symmetry solution for vacuum hohlraums with liners. Axial stagnation of the liner material at later times generated a pole-high x-ray pulse that could not be offset by raising the power of the inner beams. However, if we included a very low fill of He, 0.1mg/cc, we found we could tune the symmetry. In these simulations we again found it necessary to raise the fraction of power to the inner beam in order to tune the symmetry.

All these simulations of alternative hohlraums predict coronal electron temperatures considerably higher than the ~4.5keV temperature in the He filled design, shown in figure 8. For example, the targets filled with SiO_2 foam have T_e ~7keV. Higher temperature reduces the filamentation figure of merit, equation 1, and, in principle, makes such hohlraums less likely to suffer from filamentation. However, increased resistance to filamentation allows one to contemplate higher laser intensity and, therefore, higher radiation temperature designs. Thus, hohlraums with compositions other than the conventional He or He:H in the beam path may be a pathway to higher radiation temperatures with 2ω.

These few preliminary simulations of alternative hohlraums are far from being detailed point designs. However, they do show that it is possible to consider replacing the He or He-H gas of the conventional NIF designs with some other material and still be able to produce the required drive and adequate symmetry for ignition. This, in turns, means that it could be possible to engineer LPI in 2ω (or, even, 3ω) ignition designs by engineering the plasma composition in the beam paths. Alternative hohlraums are a new area of investigation that we will be examining in the coming years.

References:

1- J. A. Paisner, E. M. Campbell and W. J. Hogan, Fusion Technol. **26**, 755 (1994)

2- R. S. Craxton, "Theory of high-efficiency third harmonic generation of high-power Nd-glass radiation." Opt. Commun. 34, 474-478 (1980).; B. M. Van Wonterghem et. al. , Appl. Opt. 36, 4932 (1997).

3- K. Manes, M. Spaeth, LLNL, private communication, 2003.

4- L. Suter, J. Rothenberg, D. Munro, B. Van Wonterghem and S. Haan, Phys. Plasmas 7, 2092 (2000).

5- J. D. Lindl, Phys. Plasmas **2**, 3933 (1995).

6- T. Dittrich, S. W. Haan, M. M. Marinak, S. M. Pollaine, and R. McEachern, Phys. Plasmas 5, 3708 (1998).

7- S.W. Haan, T. Dittrich, G. Strobel, S. Hatchett, D. Hinkel, M. Marinak, D. Munro, O. Jones, S. Pollaine, and L. Suter, "Update on ignition target fabrication specifications," *Fusion Science and Tech*. **41**, 165 (2002); G. Strobel, S. W. Haan, et. al. Submitted for publication.

8- See National Technical Informantion service Document No. DE96010473, 1996 ("Special Issue: *Nova Technical Contract"*, ICF Quarterly Report, July-September 1995, p. 209 (UCRL-LR-105821-95-4)). Copies man be ordered from the National Technical Information service, Springield, VA 22161.

9- L. J. Suter, A. A. Hauer, L. V. Powers, *et. al.,* Phys. Rev. Lett. 73, 2328 (1994).

10- T. J. Orzechowski, M. D. Rosen, H. N. Kornblum, et. al., Phys. Rev. Lett. 77, 3545 (1996).

11- D. Colombant, M. Klapisch and A. Bar-Shalom, Phys. Rev. E 57, 3411 (1998).

12- H. Nishimura, T. Endo, H. Shiraga, Y. Kato and S. Nakai, Appl. Phys. Lett. 62, 1344 (1993).

13- S. W. Haan, S. M. Pollaine, J. D. Lindl *et. al.,* Phys. Plasmas 2, 2480 (1995).

14- W. J. Krauser, N. M. Hoffman, D. C. Wilson, *et. al.,* Phys. Plasmas 3, 2084 (1996).

15- B. J. MacGowan, B. B. Afeyan, C. A. Back, R. L. Berger, Phys. Plasmas 3, 2029 (1996).

16- S. H. Glenzer, L. J. Suter, R. E. Turner, *et. al.*, Phys. Rev. Lett. 80, 2845-2848 (1998),

17- J. D. Moody, B. J. MacGowan, J. E. Rothenberg, *et. al.,* Rev. Lett. 86, 2810-2813 (2001)

18- E. A. Williams, LLNL, private communication (1999).

19- M.J. Norman, J.E. Andrew, T.H. Bett *et al,* Appl. Opt. **41** , 3497 (2002)

20- J. M. Soures, R. L. McCrory, C. P. Verdon *et al.,* Phys. Plasmas 3,3108 (1996)

21- A. MacKinnon, LLNL, private communication (2003).

22- J. Moody, Proceedings of the Third International Conference of Inertial Fusion Sciences and Applications, Monterey, CA, 2003, edited by H. Azechi, B. Hammel, D. Meyerhoffer, J. Meyer-ter-Vehn (American Nuclear Society, Scientific Publication Department. LaGrange Park, IL, 2004).

23- C. H. Still, R. L. Berger, A. B. Langdon, *et. al.,* Phys. Plasmas, **7**, 2023 (2000).

24- M. Stevenson, Phys. Plasmas, 2004 (to be published)

25- M. M. Marinak, G. D. Kerbel, N. A. Gentile, *et al,* Phys. Plasmas, **8**, 2275 (2001)

26- N. Meezan, Proceedings of the Third International Conference of Inertial Fusion Sciences and Applications, Monterey, CA, 2003, edited by H. Azechi, B. Hammel, D. Meyerhoffer, J. Meyer-ter-Vehn (American Nuclear Society, Scientific Publication Department. LaGrange Park, IL, 2004).

27- D.S. Montgomery, B.B. Afeyan, J.A Cobble *et al*, Phys. Of Plasmas,.**5**, 1973 (1998)

Figure captions

Figure 1- Current estimates of NIF's maximum 1ω output power as a function of 1ω extracted energy, assuming all seven "slots" in the final, booster amplifiers are loaded with slabs of neodynium glass.

Figure 2- Potential NIF target design space with 2ω. The light (darker) shaded areas show all combinations of NIF energy and capsule absorbed energy potentially available with 2ω at 250eV (300eV) peak radiation temperature. Both of these are very much larger than the design space we envisioned when we began NIF, indicated by the dark triangle.

Figure 3- X-ray power absorbed by a 600kJ, 250eV graded dopant Be capsule vs. time.

Figure 4- Upper bound on design space for 250eV (top) and 300eV (bottom) peak radiation temperatures for 1ω to 2ω conversion efficiencies, η_{1-2}, ranging between 50 and 90%.

Figure 5- 250eV 2ω ignition targets modeled with integrated 2D Lasnex. simulations. Top: An ~1cm diameter hohlraum with an ~4mm diameter Be capsule absorbing 850 kJ of x-rays. Standard, 3.65 case:capsule ratio. Bottom: An ~1.1cm diameter hohlraum with an ~3mm diameter Be capsule absorbing 400 kJ of x-rays. 5:1 case:capsule ratio. These simulated hohlraums have rotational symmetry around the z-axis and left right symmetry around the midplane (r-axis).

Figure 6- Pulse shapes required for the 3.65:1 (solid) and 5:1 (broken) case:capsule ratios. Energy in solid (broken) curve is 3.4 MJ (3.3 MJ).

Figure 7- Hotspot shape at ignition time from the integrated simulations. Both produce near 1-D yield. Left (Right) is the 850 kJ (400kJ) capsule in a hohlraum of case:capsule ratio 3.65:1 (5:1). The bright material is cold, dense DT ice, the dark material inside the ice is the hotspot.

Figure 8- Plasma conditions from integrated simulations of the 3.65 case:capsule ratio target, at 1ns after peak power. Top for the outer cones, bottom for the inner cones.

Figure 9- 2ω Raman and Brillouin reflectivity as a function of intensity. Omega gasbags filled with 0.12 n_c of hydrocarbon gas. 250 eV ignition hohlraums can operate at a peak outer (inner) quad intensity of ~ $3x10^{14}$ ($1.5x10^{14}$) w/cm^2.

Figure 10- Raman and Brillouin backscatter as a function of composition, ordered in increasing average atomic number, Z. Black bars are Helen data. Grey bars are Omega data. Plasma composition influences backscatter far more than was previously thought

Figure 1

Figure 2

Figure 3

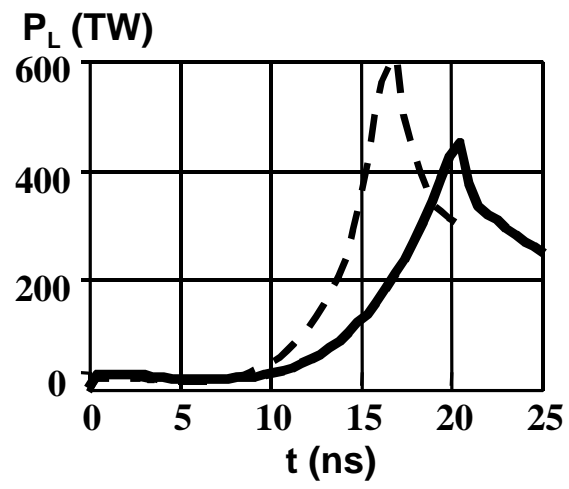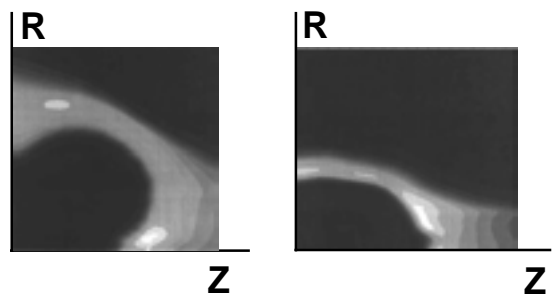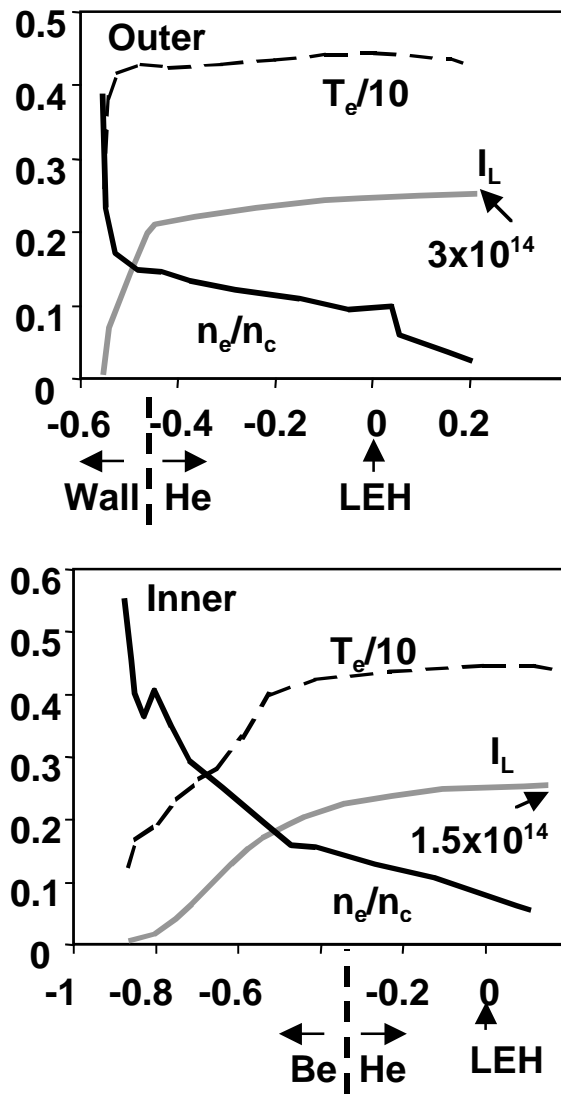
P_{cap0} (TW)
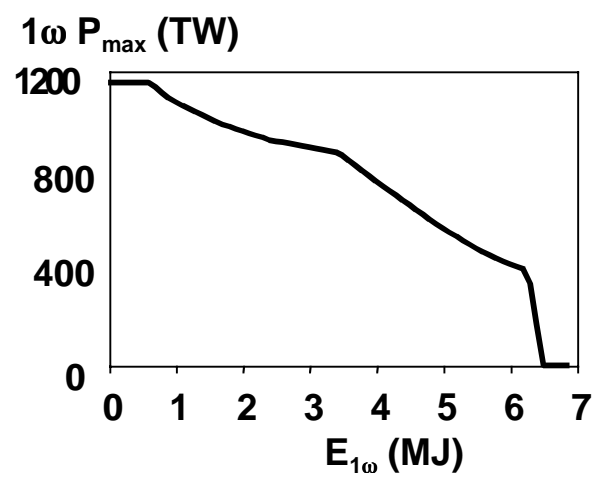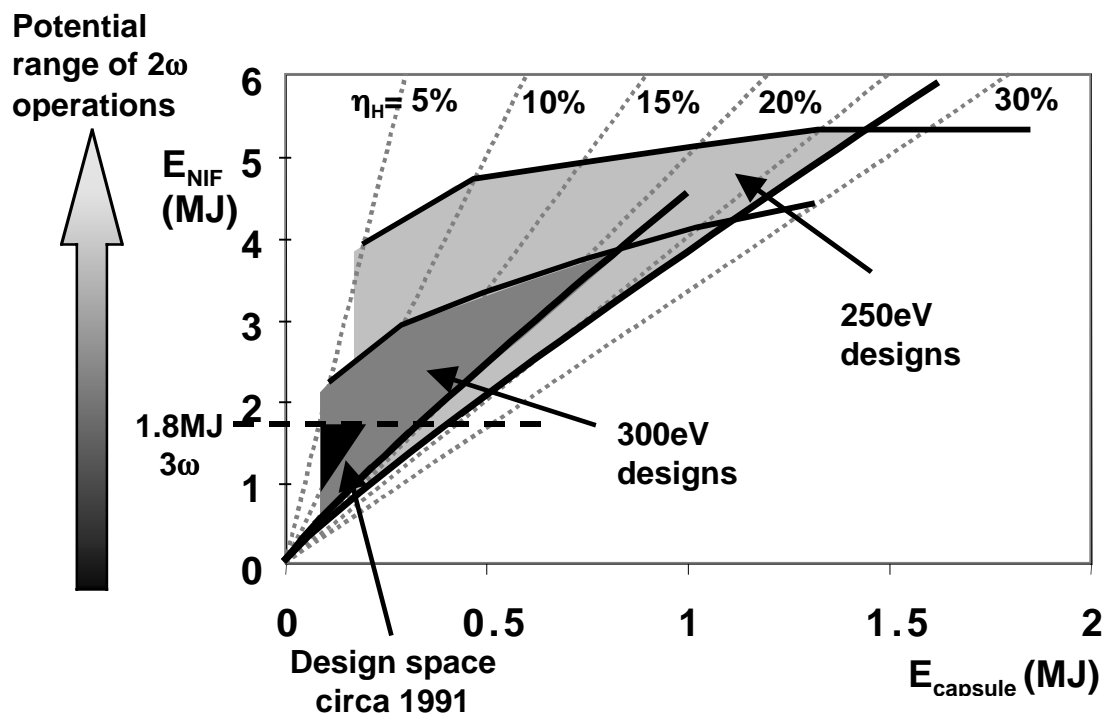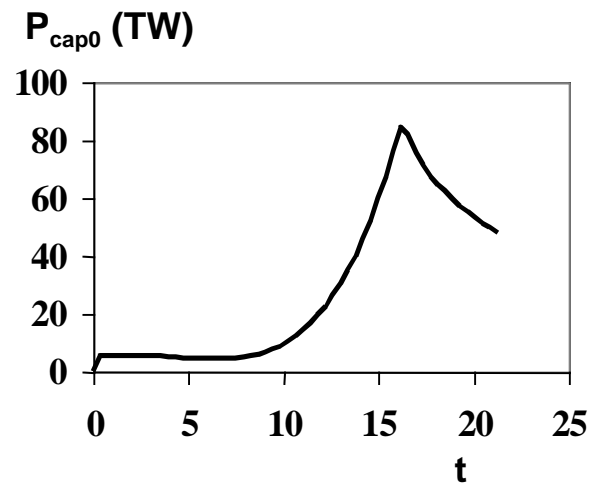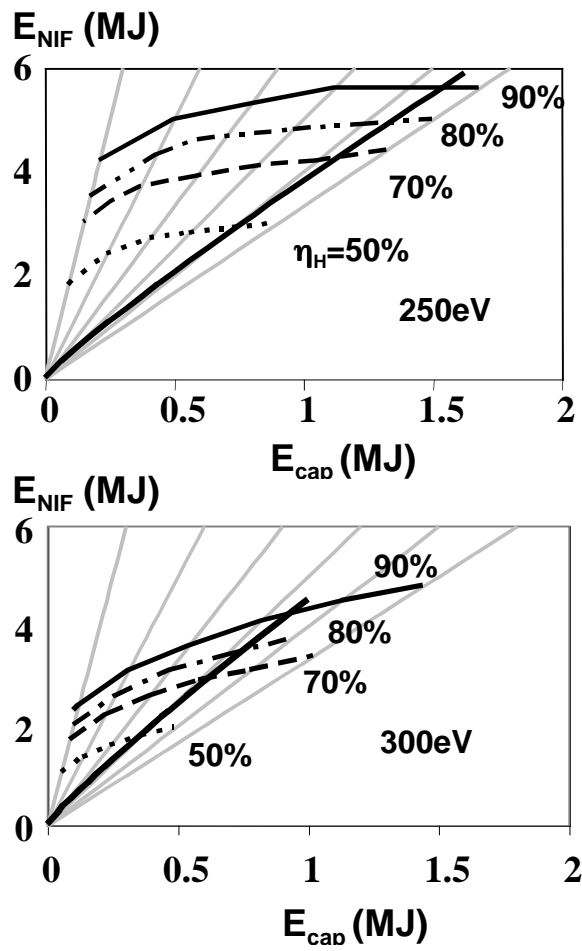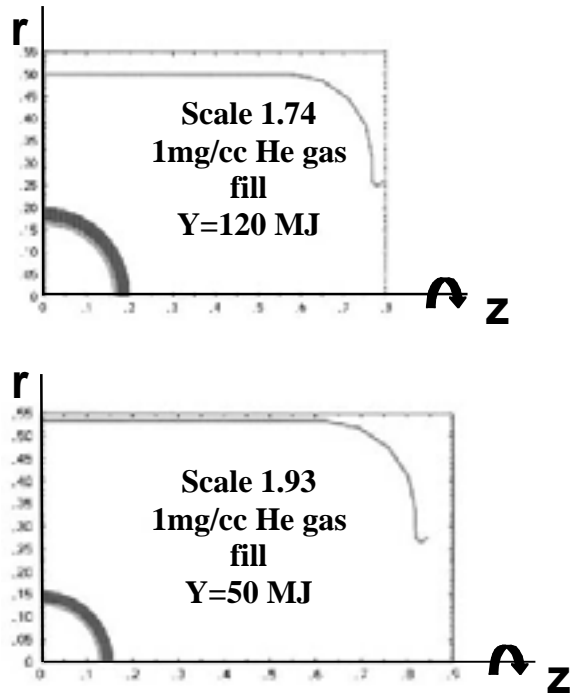
Figure 4

Figure 5

Figure 6

Figure 7

Figure 8

Figure 9

Figure 10